Degree project

UNIVERSITY OF SKÖVDE

Molecular detection of *Sclerotinia sclerotiorum* from petals of oilseed rape by Nanopore sequencing using MinIon

Master Degree Project in Bioscience

Second Cycle 30 credits

Spring term 2023

Student: Sohunda Abela
a22sohab@student.his.se

Supervisor: Maria Algerin
maria.algerin@his.se

Examiner: Magnus Fagerlind
magnus.fagerlind@his.se

Abstract

Sclerotinia sclerotiorum is a plant pathogenic fungus that causes Sclerotinia stem rot in oilseed rape. In Sweden, the disease causes severe crop loss that varies by year. Previous studies have shown a relationship between the proportion of infected petals and disease incidence in infected fields in places with high humidity levels before and during flowering. In this study, the aim was to develop a technique to detect *S. sclerotiorum* and other fungi pathogens in the petals of oilseed rape from naturally infected fields by using nanopore sequencing from Oxford Nanopore Technologies. DNA was extracted from the petals of oilseed rape and subsequently amplified by performing PCR after optimizing the optimal annealing temperature. Using the forward primer ITS1catta and the reverse primer ITS4ngsUni, these primers targeted the ITS region, which is used as a marker for the identification of fungi. The resulting Amplicon concentrations varied. Five amplicon PCR samples were selected for MinION sequencing. These samples were selected since they had the best purity levels. Finally, bioinformatic analysis was done with Kraken2 and the Pavian tool and compared with UNITE databases. The result showed hundreds of thousands of reads were recovered from the Ascomycota and Basidiomycota fungi divisions; *S. sclerotiorum* was observed in one field sample; other Sclerotiniaceae species like *Dumontinia tuberosa*, *Botrytis cinerea*, and *Sclerotinia bulborum* were detected in two fields; and many other fungal pathogen species affecting rapeseed crops in Sweden were successfully detected. MinION was successful in identifying *S. sclerotiorum* and other plant pathogens.

Popular scientific summary

Sclerotinia sclerotiorum is a plant pathogenic fungus that has a wide host range and geographical distribution, making it one of the most common plant pathogens. *S. sclerotiorum* can persist in the soil as sclerotia, which are black resting structures. It can live for long periods in the soil and serve as a source of inoculum for new infections. Sclerotia can germinate mycelially and directly infect plants. Another way of infection is that when the sclerotia is in the soil, it might begin to grow and produce apothecia. Later, the apothecia develop spores (ascospores), which might settle on the petals and leaves and cause an infection in the crop. *Sclerotinia* infection in oilseed rape crops is most often caused by ascospore-infected petals clinging to leaves, allowing the pathogen to penetrate the petiole and infect the stem. The infection by this pathogen causes significant losses and affects vital commercial crops. This leads the farmers to spray fungicides to reduce the losses resulting from this fungus. However, routine spraying to defend against *S. sclerotiorum* infection is not desired because infection occurs only when ascospores are released and meteorological conditions are favorable.

Identifying whether the field is infected with this fungus before spraying will be beneficial to farmers in terms of reducing the use of chemicals and also benefiting from the cost of spraying with fungicides. The aim was to identify *S. sclerotiorum* and other plant pathogens. The PCR technique amplified specific sections of the ITS region using primers ITS1catta and ITS4ngsUni, which bind to the top and bottom regions, respectively. The ITS region serves as a genetic marker for fungi. It is located between the small subunit (18S rRNA) and large subunit (28S rRNA) within the ribosomal RNA gene cluster. The ITS region typically ranges from 400 to 900 base pairs (bp) in length. It is composed of two subregions, ITS1 and ITS2, which are separated by the 5.8S rRNA gene. The ITS1 and ITS2 regions contain valuable information for fungal identification and phylogenetic analysis.

Sequencing techniques were used to determine the specific length and sequence composition of the ITS region in different fungi. The resulting amplicons from the PCR were run on gel electrophoresis and compared with a 100-bp molecular-weight DNA ladder. The PCR products were sequenced using a Nanopore sequencing MinIon device from Oxford Nanopore Technologies to confirm the presence of fungal DNA in the samples.

For the bioinformatics analysis, Kraken2 and Pavian tools were used to examine the sequences generated by MinION sequencing. The result of the analysis showed observation of the targeted fungus, *S. sclerotiorum,* in one field sample. Also, other *Sclerotinia* sp. were observed, in addition to many other fungal species and other pathogens within the phyla Ascomycota and Basidiomycota. These pathogens were found in all field samples that were analyzed.

.

Abbreviations

DNA	Deoxyribo Nucleic acid
dsDNA	Double-stranded DNA
HTS	High-throughput sequencing
ITS	Internal transcribed spacer
LSU	Large subunit
MAGs	Metagenome-assembled genomes
NCBI	National Centre or Biotechnology Information
NGS	Next-generation sequencing
NR	Nuclear ribosomal
ONT	Oxford nanopore Technology
ORF1	Open reading frame 1
PCR	Polymerase chain reaction
qPCR	quantitative PCR
RNA	Ribonucleic acid
rRNA	Ribosomal RNA
SGS	Second-generation sequencing
SSD	Solid-state drive
SSU	Small subunit

Contents

Introduction

Rapeseed, belonging to the Brassicaceae plant family, holds the distinction of being the world's third-largest source of vegetable oil, following soybeans and palm oil (Gunstone, 2001). It has a long history of cultivation by humans, particularly in cool climates, making it a valuable crop. With species such as *Brassica rapa* and *Brassica napus*, rapeseed is known for its high oil content, contributing to its economic significance. Its adaptability allows for cultivation in diverse environments across the globe (Coughlan et al., 2022).

Rapeseed is primarily cultivated for its oil, which finds applications in both the food and industrial sectors, including polymers, hydraulic fluids, and lubricants. The byproduct of oil extraction, known as rapeseed meal, is a valuable high-protein animal feed. The processing of rapeseed takes into account both the oil and the meal (O'Brien, 2008). Rapeseed oil is recognized as a "healthy oil" with potential health benefits. It is rich in monounsaturated fatty acids and polyunsaturated fatty acids, including omega-9 (oleic acid), omega-6 (linoleic acid), and omega-3 (alpha-linolenic acid) fatty acids. Additionally, rapeseed oil contains plant sterols, carotenoids (pro-vitamin A, present in cold-pressed oil), vitamin K, and tocopherols (vitamin E). The main health advantages associated with rapeseed oil include lower cholesterol levels and improved cardiovascular protection (Gül and Amar, 2006; Lin et al., 2013).

Sclerotinia sclerotiorum is a pathogenic plant fungus that infects plants and causes a disease called white mold when found in moist and cool conditions (Willets & Wong, 1980). This disease is also known as stem rot, watery soft rot, and cotton rot, which is a serious and economically destructive disease in Sweden and around the world. Diseases caused by plant pathogens such as bacteria, fungi, and viruses have been persistently leading to food losses around the world. While global demand for food continues to grow linearly with an increasing human population, agricultural productivity has been declining for a variety of reasons, including a decline in food security (Savary et al., 2012). *S. sclerotiorum* is a necrotrophic, phytopathogenic fungus that can infect over 400 plant types. Oilseed rape, tobacco, sunflower, and vegetables such as lettuce, cabbage, potato, and cauliflower are among the crops impacted by *S. sclerotiorum* (Clarkson et al., 2003). Rapid disease identification is critical for reducing losses caused by these diseases and making agriculture more sustainable (Fang & Ramasamy, 2015). Bolton et al. (2006) discuss the infection process in detail in the pathogen profile review. Sclerotia can germinate at temperatures of 7–24 °C and with high soil humidity, persisting for at least 10 days without drying (Clarkson et al., 2003). Sclerotia germinate only on the surface of the soil or within a maximum depth of 5 cm. In the autumn, sclerotia can germinate mycelially and infect plants directly. However, this direct infection is less common compared to indirect infection when they can start to grow and produce apothecia. The apothecia later produce spores (ascospores) that can land on the petals and leaves and later start an infection in the crop. After landing on the leaves of oilseed rape, these ascospores can germinate in 3 hours and generate spreading hyphae in 30 hours (Jamaux et al., 1995). Ascospores require senescent tissues or pollen as a nutrition supply for the disease's later growth (Clarkson et al., 2003).

The pathogen enters the petiole and infects the stem mostly when ascospore-infected petals fall and adhere to the leaves, but the infection can also start directly from the leaves. Once an infection is established, the pathogen has easy access to the lower stem or roots, branches, branchlets, and

pods and can then kill the entire plant (Almquist & Wallenhammar, 2014; Qin et al., 2011). Weather patterns and the time of ascospore release determine the severity of sclerotinia stem rot (Heran et al., 1999). According to McCartney et al. (2001), there is a direct relationship between the percentage of infected petals of flowers and the disease incidence of *S. sclerotiorum*. This suggests that as the percentage of infected petals increases, the overall disease incidence caused by *S. sclerotiorum* also increases. The study likely provides evidence supporting this relationship, indicating that monitoring the percentage of infected petals can serve as an indicator of the disease severity or prevalence caused by *S. sclerotiorum*. As a result, accurate monitoring of the ascospore release flower during the early flowering stage is critical for estimating disease potential (Gugel & Morrall, 1986).

In central Sweden, stem rot causes serious damage that fluctuates from year to year, and oilseed rape fields are currently treated with extensive chemical treatment (Twengstrom et al., 1998). The disease forecasting service offered to Swedish farmers is a regional risk assessment based on local weather and field data, with knowledge of disease incidence in the previous oilseed rape crop in the particular area being the most crucial element (Twengstrom et al., 1998). Based on three primary parameters such as crop rotation, weather, and the economy SkleroPro, a German forecasting model for sclerotinia stem rot in winter oilseed rape, offers recommendations for fungicide treatments (Koch et al., 2007). Many authors (Turkington et al., 1991) state that the agar petal test method can predict the occurrence of the white mold of rape. Unfortunately, it's time-consuming. Molecular biology techniques are frequently more effective at detecting plant pathogens. Fungal molecular identification by DNA barcoding has become a crucial component of fungal research. Environmental barcoding has gained popularity over the past few years because it allows for the study of fungi abundance and species richness at a more rapid and accurate rate than traditional biotic surveys, such as fingerprinting methods based on banding patterns obtained from restriction site polymorphisms or denaturing gradient gel electrophoresis profiles (Martin & Rygiewicz, 2005). For fungi, the internal transcribed spacer (ITS) of nuclear DNA (nrDNA) is the preferred DNA barcoding marker for identifying single species as well as mixed environmental templates (environmental DNA barcoding) (Martin & Rygiewicz, 2005).

Traditionally, the detection of fungi relied on selective culture media and labor-intensive immunological and biochemical tests. However, the effectiveness of these methods often depended on the cultivability of the target organism (Lievens et al., 2006). Lefol and Morrall (1996) employed immunofluorescence to detect ascospores, but this approach necessitated time-consuming microscopic examination of the petals. Bom and Boland (2000) found limited correlation between ELISA absorbance and petal infestation or disease, partly due to the inadequate specificity of the tested polyclonal antibodies.

In a previous study conducted in 1998 and 1999, researchers explored three different approaches to detect S. sclerotiorum. These methods included using two commercially available serological kits to identify inoculum on petals and employing a traditional petal test on agar. However, the results obtained from the serological kits did not align with those obtained from the agar test. The agar test, which provided a quantitative measure, was utilized to predict the risk of future disease outbreaks. A correlation was discovered between the percentage of infected petals and the incidence of disease in the field. This relationship was observed in areas characterized by high humidity before and during flowering. Conversely, fields experiencing dry weather conditions during flowering exhibited lower disease incidence, even when a high proportion of petals were infected (Wallenhammar et al., 2007). Hence, evaluating the level of inoculum present on petals

can aid in predicting the fields where chemical treatments may be warranted under specific conditions. This approach allows for targeted interventions to mitigate disease risks.

Several PCR techniques have been developed for the detection of *S. sclerotiorum.* For instance, Freeman et al. (2002) introduced a touchdown PCR method that utilizes primers targeting the internal transcribed spacer (ITS) region of *S. sclerotiorum* ribosomal DNA. This technique can be applied to air samples and oilseed rape petals inoculated with the pathogen. In another study, Rogers et al. (2009) developed a quantitative PCR technique using SYBR Green dye. This method quantifies the amount of *S. sclerotiorum* DNA collected from spore traps by targeting a specific region of a gene encoding the mitochondrial small subunit rRNA intron and ORF1. Qin et al. (2011) presented a nested PCR approach that amplifies the ribosomal ITS sequence of *S. sclerotiorum*. Nested PCR involves two rounds of amplification, with the first round generating a larger DNA fragment and the second round targeting a smaller, specific region within the initial fragment. Additionally, Abd-Elmagid et al. (2013) developed a multiplex conventional PCR assay capable of distinguishing four *Sclerotinia species*, including *S. sclerotiorum*. This multiplex PCR technique enables the simultaneous amplification of multiple target DNA sequences using specific primer sets.

In regions where high humidity prevails before and during flowering, a correlation has been observed between the proportion of infected petals and disease incidence in the field. Conversely, in areas characterized by dry weather during flowering, fields with high levels of infected petals have shown low disease incidence (Wallenhammar et al., 2007). Therefore, in certain circumstances, assessing the amount of inoculum on petals can be a valuable technique for identifying fields that would benefit from a chemical treatment (Wallenhammar et al., 2012). White et al. (1990) introduced the use of fungal nuclear ribosomal operon primers as a DNA molecular method for fungal identification. These primers were designed to target the large subunit (LSU), small subunit (SSU), and the entire internal transcribed spacer region (ITS, 5.8S, and ITS2) of the ribosomal DNA. In eukaryotes, the genes responsible for encoding ribosomal RNA (rRNA) and the spacers between them are often arranged as tandem repeats. This unique characteristic led to the selection of the Internal Transcribed Spacer (ITS) region as the official barcode for fungi by a consortium of mycologists (Schoch, 2012). The ITS region is situated between the small subunit (18S rRNA) and large subunit (28S rRNA) within the ribosomal RNA gene cluster. It consists of two subunits, namely ITS1 and ITS2, which are separated by the 5.8S rRNA gene. The length of the ITS region can vary significantly among different lineages, typically ranging from 400 to 900 base pairs (bp). Each subunit, ITS1 and ITS2, generally spans 250 to 400 bp in length, while the 5.8S unit is located in between (Kress et al., 2012; Wurzbacher et al., 2019). This specific region has been defined as a barcode identifier within the ribosomal tandem repeat gene cluster of the nuclear genome and has proven to be valuable for fungal species identification and differentiation.

DNA barcoding utilizes a short, standardized region of DNA to compare with a reference library of similar DNA sequences, enabling the identification of species. The DNA barcoding approach, using the ribosomal ITS region, can be employed for specific identification of organisms or species (Kress et al., 2012). However, the efficiency of cataloging and identifying specimens in DNA barcoding is influenced by the universality of PCR primers, making the selection of high-coverage barcoding primers crucial (Bellemain et al., 2010). Loit et al. (2019) found that the ITS1catta-ITS4ngsUni primer pair predominantly amplified fungal DNA, accounting for 99.9% of the detected reads. The ITS1catta primer covers a wide range of Ascomycota and Basidiomycota, as

well as selected groups of zygomycetes and early diverging lineages. However, it excludes plants and the majority of other eukaryote groups, including fungal taxa such as Mortierellomycota and Tulasnellaceae (Loit et al., 2019). Third-generation high-throughput sequencing (HTS) technologies, capable of sequencing single DNA molecules, have the ability to recover diverse alleles and pseudogenes from mixed or contaminated materials (Cornelis et al., 2019).

The MinION is a third-generation sequencing technology that uses a nanopore-based method to generate lengthy reads of up to hundreds of thousands of bases (Goldstein et al., 2019; Jansen et al., 2017; Pennisi, 2012; Reiner et al., 2012). In comparison to previous HTS platforms, which were represented by massive and expensive machines, it is considered the smallest sequencing device currently available, and costs the same as a computer, making it affordable to governmental organizations, research laboratories, and small businesses (Mikheyev & Tin, 2014). MinION measuring only 10 × 3 × 2 cm and weighing only 90 g (Figure 1). It can be plugged straight into a normal USB3 port on a computer, requiring little gear and little setup. MinKNOW is specialized software that runs on the host computer to which the MinION is connected.

The first step of sequencing is library preparation, which is minimal, involving only fragmentation of DNA and ligation of adapters; PCR is optional. Both strands of DNA should be used, which means sequencing of both strands can be done. A voltage can be supplied to the membrane with nanopores to force DNA through the pore, and an ion current flow can be measured. When a DNA molecule passes through the nanopore, the current pattern or magnitude changes, which may be observed and described. A sensor measures the current in the nanopore thousands of times per second, and the data streams are sent to a microprocessor known as the application-specific integrated circuit. Finally, data processing is handled by the MinKNOW software, which is responsible for data collection and analysis (Ip et al., 2015).

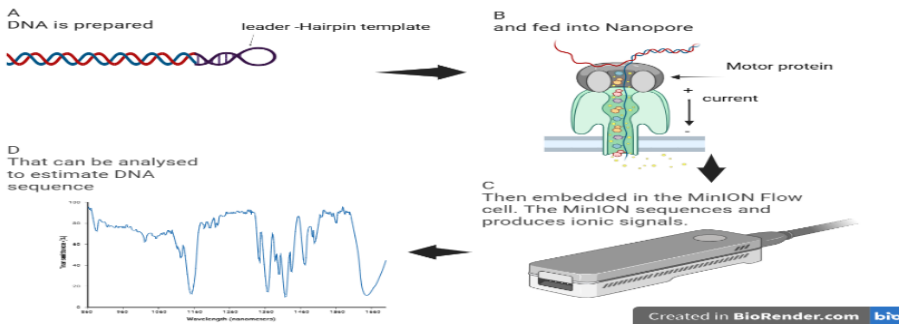

Figure 1. Image showing the MinION device and the principle of Nanopore sequencing. Created with BioRender.com. The leader sequence interacts with the pore and motor protein to direct DNA, a hairpin allows for biodirectional sequencing (A). During sequencing, a helicase enzyme denatures double-stranded DNA by dragging one DNA strand through one of the nanopores contained in the synthetic membrane, across which a voltage is continuously applied (B). As the ssDNA flows through the nanopore, the different bases restrict ionic flow in a precise manner (C), allowing the molecule to be sequenced by sensing characteristic variations in voltage at each channel, meaning sequencing happens in real-time(D).

Aim and objectives

Aim

This study aims to develop a method to detect *S. sclerotiorum* and other fungal pathogens in the petals of oilseed rape from seven naturally infected fields by using the nanopore sequencing device MinIon from Oxford Nanopore Technologies.

Objectives

- Isolate genomic DNA from petals collected from naturally infected oilseed rape fields.
- Using PCR and the appropriate primers in combination to amplify the ITS region of the isolated DNA.
- Perform MinIon sequencing to sequence the barcode ITS genes of *S. sclerotiorum* and other fungi pathogens detected in the various petal samples and compare them with reference sequences.

Materials and methods

Biological materials, oilseed rape petals

The biological samples for this study were collected from seven different naturally infected fields in Sweden with different percentages of infection, Ova 10%, Kaflås 5%, Dala 6%, Hovby 25%, Grevbäck 8%, Forsby8%, and Vinninga11%, (20 inflorescences sample per field). The oilseed rape fields were situated in the northeastern part of Västra Götaland. The petals were kept in a freezer at 20°C.

DNA Extraction from Petals

The DNA from each petal was extracted using a commercial lysis buffer, MicroLYSIS-PLUS (Microzone Ltd.), according to a modified protocol as described by Almquist and Wallenhammar (2014). The DNA pellet was left to air-dry before resuspension in 30 µl of sterile milli-Q water. The twenty DNA samples from each field were pooled into one sample; only seven were subsequently used to run PCR. After DNA extraction, the samples were treated with RNAse A (Omega Bio-Tek) to remove RNA from the samples (1 µl RNAse A + 20 µl of DNA). The stock concentration of RNAse A was 25 mg/mL, and it was incubated for 1 hour at 37 °C. Then to determine the purity of DNA samples, the absorbance ratios of $A_{260}/_{280}$ and $A_{260}/_{230}$ were measured using a DeNovix DS-11 spectrophotometer (DeNovix Inc). The DNA quantification was performed both before and after treatment with RNAse A using the Invitrogen Qubit™ 4 fluorometer and the dsDNA HS assay kit from Thermo Fisher Scientific.

PCR amplification

PCR reaction was performed by using the forward primer ITS1catta (5′-ACCWGCGGARGGATCATTA-3′) and the reverse primer ITS4ngsUni (5′-CCTSCSCTTANTDATATGC-3′). During the optimization process, an error occurred where only one specific sample was loaded for each temperature instead of testing all samples at every

temperature. Following the supervisor's advice, it was determined that using only one temperature yielded the brightest bands for all samples. As the optimization process cannot be repeated at this stage, it was recommended to omit mentioning it in the report. The selection of temperatures was based on a previous thesis conducted by another student. The annealing temperature was set at 58.5 °C. The PCR amplification was performed using the Thermo Scientific™ Phusion™ Hot Start II High-Fidelity DNA polymerase kit, and DNA extracted from all petal samples was used for the PCR amplification and was performed in a 50-µL reaction mixture (Table 1). PCR was run for several attempts by changing the cycle nuber from 35 until reaching 40 cyles, so the final PCR settings were: initial denaturation at 98 °C for the 30s, followed by 40 cycles of 98 °C for 10 s (denaturation), varying (The annealing temperature for PCR was set at 58.5 °C) for 30 s (annealing), 72 °C for 60 s (elongation), and final extension at 72 °C for 10 minutes. Amplification was done with a BIO-RAD IPTC-200 thermal cycle.

Table 1. PCR optimization, 50-µl reaction

Components	**Final concentrations used for the PCR**	**Final volume (µl)**
5X Phusion buffer	1 X	10
dNTP 10 mM	200 µM	1
Forward Primer 10 µM	0.5 µM	2.5
Reverse primer 10 µM	0.5 µM	2.5
Template DNA	10 ng	5
Phusion Hot Start II DNA polymerase (2U/µl)	1 U	0.5
H_2O	-	28.5

DNA samples were diluted to 2 ng/µl after measuring the concentrations.

Gel electrophoresis

The resulting amplicons (10 µl) with 2 µl 6X purple gel loading dye (New England Biolabs) were run on an agarose gel. Moreover, a 100-bp molecular-weight DNA ladder (New England Biolabs) was loaded in the first and last wells in 1% agarose (1X TAE buffer) stained with 1X GelRed® (Biotium) at 100 volts for 1 hour.

Cleaning

The QIAquick PCR purification kit from Qiagen was used to clean the amplicons following the manufacturer's instructions. The concentration of the purified DNA was determined using the Qubit™ 4 fluorometer dsDNA HS assay kit from Thermo Fisher Scientific. The purity of the DNA was evaluated using a DeNovix DS-11 spectrophotometer (DeNovix Inc).

Nanopore sequencing

Library preparation

During the MinION sequencing process, five samples were chosen based on absorbance ratios (A_{260}/A_{280} and A_{260}/A_{230}) from the PCR products. The Native barcoding expansion kit 1–12 (EXPNBD104), ligation sequencing kit (SQK-LSK109), and protocol provided by Oxford Nanopore Technologies were employed for library preparation. For each sample, 100–200 fmol was required, with 150 fmol used, as calculated using the NEBioCalculator online tool. The library preparation protocol was followed according to the manufacturer's instructions, with some modifications. The ratio of AMPure XP beads to sample was increased to 2:1 instead of the standard 1:1 ratio. Additionally, during the native barcode ligation procedure, barcodes NB08 to NB012 were attached to the five samples (as listed in Table 2). Instead of using the TA ligase master mix, a 2X T4 DNA ligase (New England Biolabs) was prepared and utilized.

Sequencing and basecalling

All five samples were sequenced with the Spot-ON Flow R9 flow cell version from Oxford Nanopore Technologies in the laboratory at room temperature. The MinION device, also from Oxford Nanopore Technologies, was used to connect to a laptop that had the MinKNOW (ONT) software installed. Guppy command-line software was set up with high-accuracy basecalling and stored the reads in passed and failed files. Sequencing was stopped after 20 hours, and a sufficient number of sequences were obtained.

Sequence analysis

The bioinformatics analysis of the sequencing data involved the use of the Kraken2 taxonomic classification system (Wood et al., 2014) and the UNITE database to handle potential undescribed or barcoded species in the samples (Tedersoo et al., 2022). Kraken2 provide rapid taxonomic classification based on multiple best hits in metagenomics and metabarcoding (Wood et al., 2019). The UNITE database contain eukaryotic ITS data, including curated submissions from the INSDc (Nilsson et al., 2018). Sankey diagrams were generated using the Pavian tool (Ondov et al., 2011), which displayed the taxonomic classification of each sample.

Results

DNA extraction from Petals

The results of the DNA extraction and quantification techniques used in the investigation are provided in the appendices. In Appendix 1, the DNA concentrations of petals before RNAse A treatment ranged from 1.26 to 4.46 ng/µl (Qubit measurement) and from 86.2 to 283.5 ng/µl (NanoDrop measurement). The absorbance ratios of $A_{260}/_{280}$ ranged from 2.82 to 2.06, and $A_{260}/_{230}$ ranged from 0.43 to 0.86.

In Appendix 2, the DNA concentrations of samples after RNAse A treatment ranged from 0.72 to 2.10 ng/µl (Qubit measurement) and from 190.2 to 294.3 ng/µl (NanoDrop measurement). The absorbance ratios of $A_{260}/_{280}$ ranged from 1.28 to 1.77, and $A_{260}/_{230}$ ranged from 0.30 to 0.63.

PCR and gel electrophoresis

PCR reactions were conducted using DNA extracted from petal samples obtained from seven different fields. Initially, several PCR reactions were attempted, but no visible PCR products were obtained. The agarose gel analysis did not reveal any discernible bands (data not shown). To address this issue, several iterations of PCR optimization were performed to improve the amplification results. The optimization process involved adjusting various parameters such as, annealing temperatures, and cycle numbers. By systematically adjusting the PCR conditions, it was possible to refine the protocol and achieve successful amplification of the target DNA regions. The modifications implemented in the optimized PCR protocol led to visible bands of the expected sizes on the agarose gel, indicating the successful amplification of the desired DNA fragments (data not shown).

The PCR utilized the primer pair ITS1Catta and ITS4ngsUni, with an annealing temperature of 58.5°C. The resulting PCR products were visualized on an agarose gel (Figure 2). To improve the PCR yield, the cycle number was increased to 40 cycles, which deviated from the original protocol. The expected sizes of the amplicons ranged from 400 to 900 base pairs (bp). By adjusting the cycle number and using the specific primer pair, the goal was to amplify the target DNA regions within this size range.

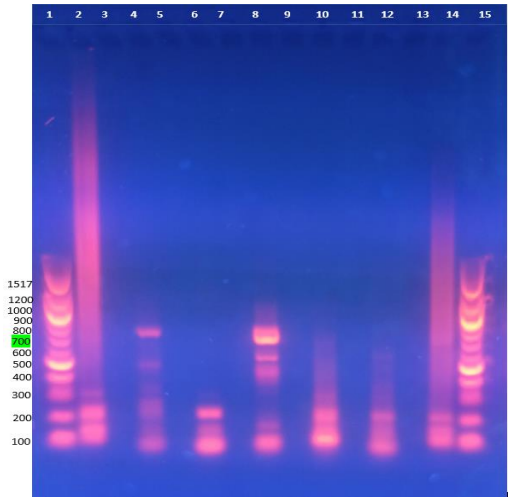

Figure 2. Gel images illustrating PCR run at 58.5 °C annealing temprature; using 7 DNA petal samples . Well numbers 1 and 15 represent the 100-bp DNA ladder (NEB Biolabs), which indicates fragment size in terms of the number of base pairs. Wells 2, 4, 6, 8, 9, 12, 14, and 15 represent 6 samples amplified with primer pairs ITS1Catta and ITS4ngsUni; wells 8–13 and 15 represent samples from Ova, Kaflås, Dala, Hovby, Grevbäck, Vinninga, and Forsby, respectively

PCR cleaning

Amplicons from PCR using primer pairs ITS1Catta and ITS4ngsUni were cleaned and quantified, and purity was determined (Table 2). For sequencing, the most pure samples ($A_{260}/_{280}$ ratio close to 1.8) were utilized. Five samples were chosen (Kaflås, Dala, Hovby, Grevbäck, and Vinninga), and barcodes were assigned.

Table 2. DNA quantification of cleaned PCR products and purity results; barcode refers to samples.

Primer pair	Fields	Absorbance 260/280	Absorbance 260/230	Qubit concentration (ng/µl)	Barcodes
ITS1Catta/ITS4ngsuni	Ova	1.27	1.06	3.86	-
	Kaflås	1.77	0.58	1.09	NBO8
	Dala	1.67	1.13	1.33	NBO9
	Hovby	1.72	1.20	4.18	NBO10
	Grevbäck	1.71	0.72	1.87	NBO11
	Vinninga	1.58	0.77	0.65	NBO12
	Forsby	1.41	2.00	4.84	-

MinION sequencing

Sequencing Performance and Data Analysis

To analyze the sequences generated by MinION sequencing, two databases, Kraken2 and UNITE, were utilized. The classification results obtained from both databases were compared. When the Kraken2 database was used for analysis, the percentage of classified data in all five samples ranged from 22% to 28%. This indicates that a portion of the sequences could be confidently assigned to specific taxonomic groups using Kraken2 (as shown in Table 3). In contrast, when the UNITE database was employed, the percentage of classified data increased for all samples, ranging from 38% to 60%. The utilization of the UNITE database allowed for a higher proportion

of the sequences to be assigned to known taxonomic groups, indicating a broader coverage of fungal taxa (as shown in Table 3).

Table 3. Shows the performance of the two databases.

Sample ID	Percentage of reads (%)	Kraken2 Database	UNITE Database
Kaflås	Classified	27.5%	40.79%
	Unclassified	72.5%	59.79%
Dala	Classified	22.2%	38.68%
	Unclassified	77.8%	61.32%
Hovby	Classified	26.8%	60.11%
	Unclassified	73.2%	39.89%
Grevbäck	Classified	24.8%	40.22%
	Unclassified	72.5%	59.78%
Vinninga	Classified	28.1%	40.03%
	Unclassified	71.9%	59.97%

The Pavian tool was employed to conduct further taxonomic analysis and classification of the sequencing data. Sankey diagrams were created using Pavian to visualize the detailed eukaryotic taxonomic classification of each sample. These diagrams provide a comprehensive overview of the taxonomic composition within each sample, showcasing the flow of taxonomic assignments.

Figures 3A–E present the Sankey diagrams generated for each sample, illustrating the eukaryotic taxonomic classification based on the Kraken2 database. Additionally, Sankey diagrams were created for the UNITE database (data not shown), encompassing all classified hits mentioned in Table 5. These diagrams offer a more detailed and visual representation of the taxonomic assignments for each sample.

To facilitate a more precise comparison of the outputs, the most abundant phyla and species were tabulated in Table 4 and Table 5, respectively. This tabulation enables a straightforward assessment of the predominant taxonomic groups and species identified in each sample, allowing for a comparative analysis across the dataset.

A.

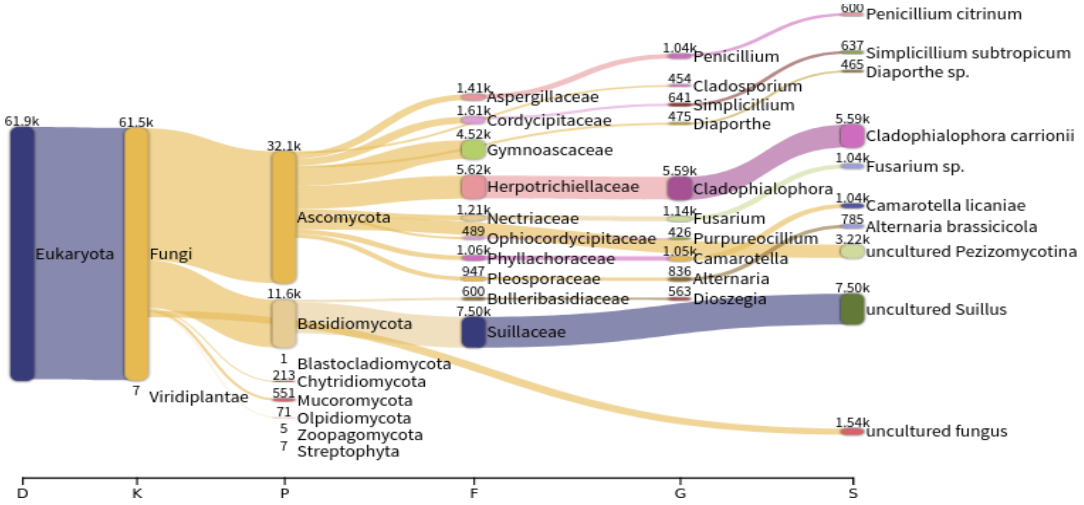
61.9k
Eukaryota
61.5k
Fungi
7
Viridiplantae
32.1k
Ascomycota
11.6k
Basidiomycota
1
Blastocladiomycota
213
Chytridiomycota
551
Mucoromycota
71
Olpidiomycota
5
Zoopagomycota
7
Streptophyta
1.41k
Aspergillaceae
1.61k
Cordycipitaceae
4.52k
Gymnoascaceae
5.62k
Herpotrichiellaceae
1.21k
Nectriaceae
489
Ophiocordycipitaceae
1.06k
Phyllachoraceae
947
Pleosporaceae
600
Bulleribasidiaceae
7.50k
Suillaceae
1.04k
Penicillium
454
Cladosporium
641
Simplicillium
475
Diaporthe
5.59k
Cladophialophora
1.14k
Fusarium
426
Purpureocillium
1.05k
Camarotella
836
Alternaria
563
Dioszegia
600
Penicillium citrinum
637
Simplicillium subtropicum
465
Diaporthe sp.
5.59k
Cladophialophora carrionii
1.04k
Fusarium sp.
1.04k
Camarotella licaniae
785
Alternaria brassicicola
3.22k
uncultured Pezizomycotina
7.50k
uncultured Suillus
1.54k
uncultured fungus
D
K
P
F
G
S

B.

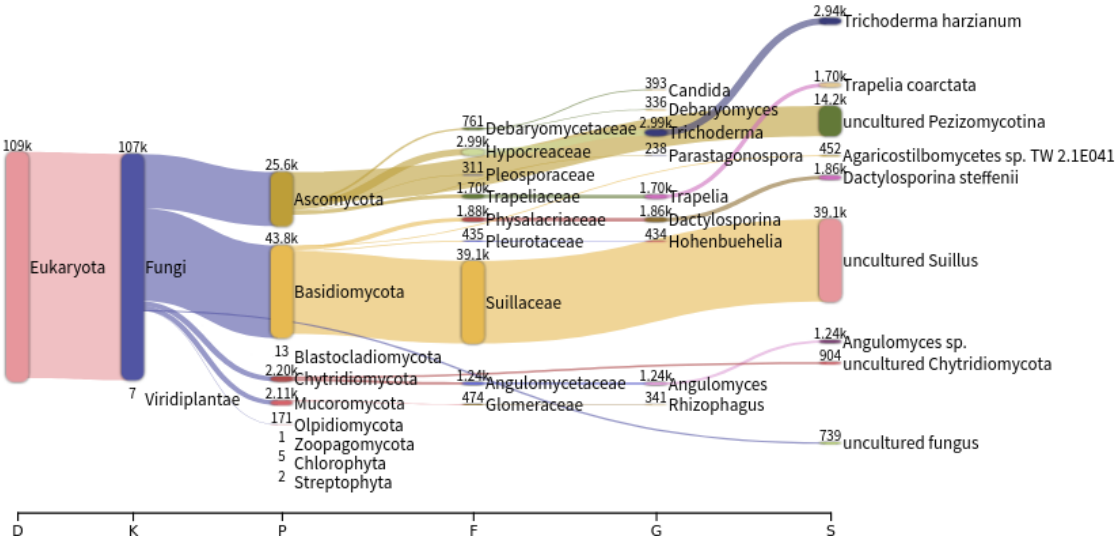
109k
Eukaryota
107k
Fungi
7
Viridiplantae
25.6k
Ascomycota
43.8k
Basidiomycota
13
Blastocladiomycota
2.20k
Chytridiomycota
2.11k
Mucoromycota
171
Olpidiomycota
1
Zoopagomycota
5
Chlorophyta
2
Streptophyta
761
Debaryomycetaceae
2.99k
Hypocreaceae
311
Pleosporaceae
1.70k
Trapeliaceae
1.88k
Physalacriaceae
435
Pleurotaceae
39.1k
Suillaceae
1.24k
Angulomycetaceae
474
Glomeraceae
393
Candida
336
Debaryomyces
2.99k
Trichoderma
238
Parastagonospora
1.70k
Trapelia
1.86k
Dactylosporina
434
Hohenbuehelia
1.24k
Angulomyces
341
Rhizophagus
2.94k
Trichoderma harzianum
1.70k
Trapelia coarctata
14.2k
uncultured Pezizomycotina
452
Agaricostilbomycetes sp. TW 2.1E041
1.86k
Dactylosporina steffenii
39.1k
uncultured Suillus
1.24k
Angulomyces sp.
904
uncultured Chytridiomycota
739
uncultured fungus
D
K
P
F
G
S

C.

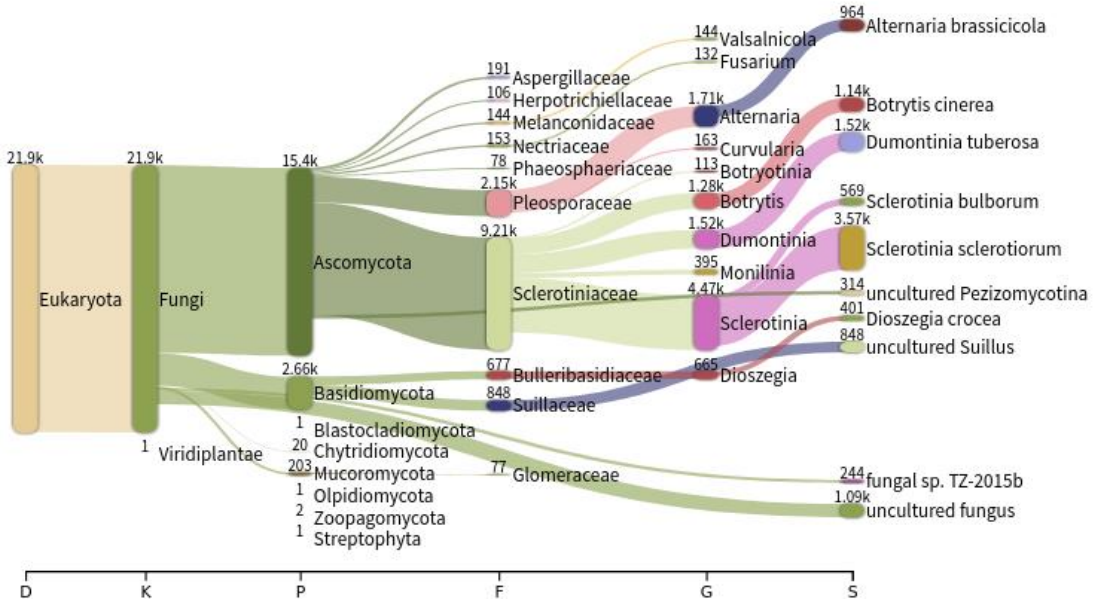
21.9k
Eukaryota
21.9k
Fungi
1
Viridiplantae
15.4k
Ascomycota
2.66k
Basidiomycota
1
Blastocladiomycota
20
Chytridiomycota
203
Mucoromycota
1
Olpidiomycota
2
Zoopagomycota
1
Streptophyta
191
Aspergillaceae
106
Herpotrichiellaceae
144
Melanconidaceae
153
Nectriaceae
78
Phaeosphaeriaceae
2.15k
Pleosporaceae
9.21k
Sclerotiniaceae
677
Bulleribasidiaceae
848
Suillaceae
77
Glomeraceae
144
Valsalnicola
132
Fusarium
1.71k
Alternaria
163
Curvularia
113
Botryotinia
1.28k
Botrytis
1.52k
Dumontinia
395
Monilinia
4.47k
Sclerotinia
665
Dioszegia
964
Alternaria brassicicola
1.14k
Botrytis cinerea
1.52k
Dumontinia tuberosa
569
Sclerotinia bulborum
3.57k
Sclerotinia sclerotiorum
314
uncultured Pezizomycotina
401
Dioszegia crocea
848
uncultured Suillus
244
fungal sp. TZ-2015b
1.09k
uncultured fungus
D
K
P
F
G
S

D.

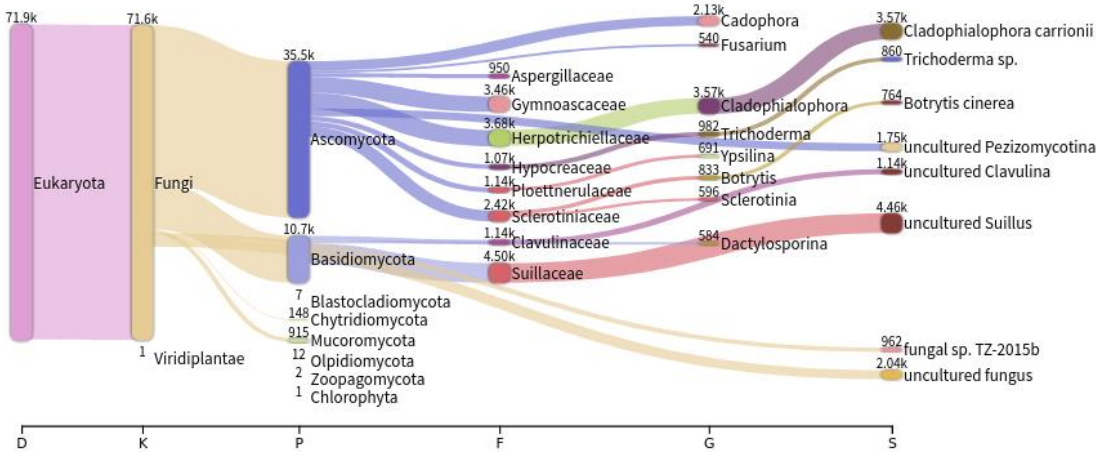
71.9k
Eukaryota
71.6k
Fungi
1
Viridiplantae
35.5k
Ascomycota
10.7k
Basidiomycota
7
Blastocladiomycota
148
Chytridiomycota
915
Mucoromycota
12
Olpidiomycota
2
Zoopagomycota
1
Chlorophyta
950
Aspergillaceae
3.46k
Gymnoascaceae
3.68k
Herpotrichiellaceae
1.07k
Hypocreaceae
1.14k
Ploettnerulaceae
2.42k
Sclerotiniaceae
1.14k
Clavulinaceae
4.50k
Suillaceae
2.13k
Cadophora
540
Fusarium
3.57k
Cladophialophora
982
Trichoderma
691
Ypsilina
833
Botrytis
596
Sclerotinia
584
Dactylosporina
3.57k
Cladophialophora carrionii
860
Trichoderma sp.
764
Botrytis cinerea
1.75k
uncultured Pezizomycotina
1.14k
uncultured Clavulina
4.46k
uncultured Suillus
962
fungal sp. TZ-2015b
2.04k
uncultured fungus
D
K
P
F
G
S

E.

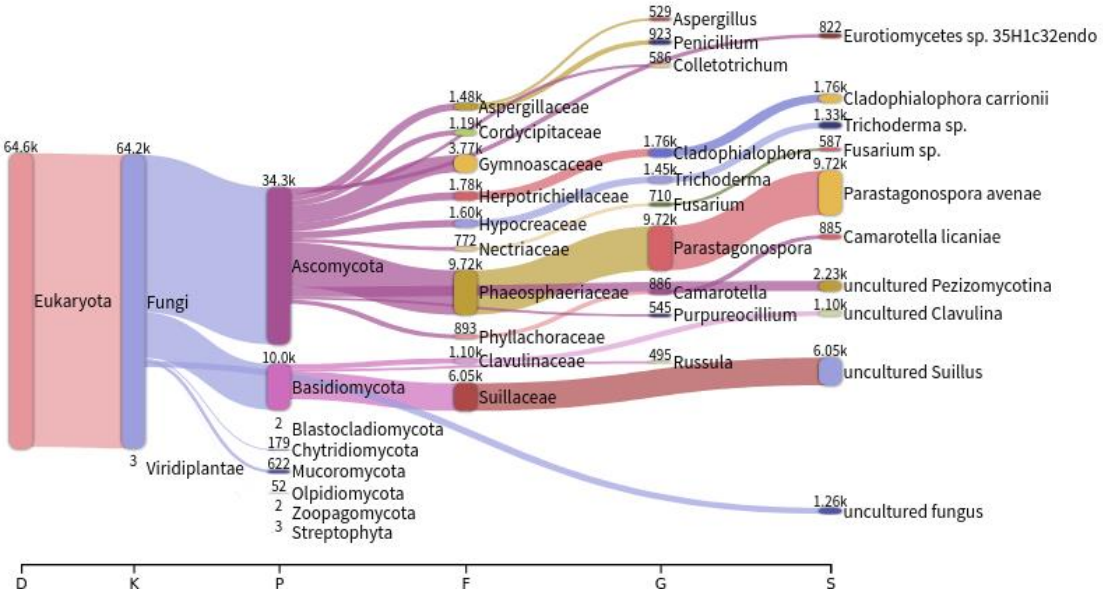

Figure 3. The taxonomic identification of Kaflås (A), Dala (B), Hovby (C), Grevbäck (D), and Vinninga (E) samples using the primer pairs ITS1Catta and ITS4ngsUni was amplified and compared to the Kraken2 Database. The results were displayed in the form of a tree, with numbers denoting the number of reads for each group and letters representing distinct taxonomic categories (D-domain, K-kingdom, P-phylum, F-family, G-genus, and S-species).

Table 4. Taxonomic identification of the samples using the Kraken2 database.

Sample ID	No. of reads obtained	No. of most abundant phyla (reads)	No. of most abundant genus/spices (reads)
Kaflås	225,157	Ascomcota 32.1 k	*Cladophialophora carrionii 5.59k*
		Basidiomycota 11.6 k	*Fusarium sp 1.04 k*
			Camarotella licaniae 1.04 k
			Alternaria brassicicola 785
			Simplicillium subtropicum 637
			Penicillium citrinum 600
			Diaporthe sp. 465
Dala	491,538	Ascomcota 25.6 k	*Trichoderma harzianum 2.94 k*
		Basidiomycota 43.8 k	*Dactylosporina steffenii 1.86 k*
			Angulomyces sp. 1.24 k
			Trapelia coarctata 1.70 k
Hovby	81,820	Ascomcota 15.4 k	*Sclerotinia sclerotiorum 3.57 k*
		Basidiomycota 266 k	*Dumontinia tuberosa 1.52 k*
			Botrytis Cinerea 1.14 k
			Alternaria brassicicola 964
			Sclerotinia bulborum 569
			Dioszegia crocea 401
Grevbäck	290,276	Ascomcota 35.5 k	*Cladophialophora carrionii 3.57k*
		Basidiomycota 10.7 k	*Trichoderma sp. 860*
			Botrytis Cinerea 764
			uncultured *Fungus 2.04*
			uncultured *Pezizomycotina 1.75k*
			uncultured *Clavulina 1.14k*
Vinninga	229,744	Ascomcota 34.3 k	*Parastagonospora avenae 9.72 k*
		Basidiomycota 10.0 k	*Cladophialophora carrionii 1.76 k*
			Trichoderma sp. 1.33 k
			Camarotella licaniae 885
			Eurotiomycetes sp 822
			Cladophialophora carrionii 1.76 k
			Trichoderma sp. 1.33 k
			Camarotella licaniae 885

For all the samples the most abundant phyla and species identified, using the UNITE database, are shown in Table 5.

Table 5. Taxonomic identification of the samples using the UNITE database.

Sample ID	No. of reads obtained	No. of most abundant phyla (reads)	No. of most abundant genus/spices (reads)
Kaflås	273,012	Ascomcota 22.9 k Basidiomycota 9.50 k	*Saccharomycodes ludwigii 15.9 k* *Sporisorium graminicola 6.13 k* *Puccinia striiformis 551* *Psilocybe cubensis 516* *Botrytis Cinerea 285* *Rhizoctonia Solani 256*
Dala	623,988	Ascomcota 27.3k Basidiomycota 28.7k	*Sporisorium graminicola 27.6 k* *Cryptococcus neoformans 1.79 k* *Puccinia striiformis 612* *Saccharomycodes ludwigii 294* *Colletotrichum higginsianum 189* *Fusarium poae 165* *Botrytis Cinerea 102*
Hovby	150,114	Ascomcota 53.4 k Basidiomycota 2.85 k	*Saccharomycodes ludwigii 33.2 k* *Botrytis Cinerea 16.5 k* *Sporisorium graminicola 616* *Cryptococcus neoformans 491* *Rhizoctonia Solani 398* *Schizosaccharomyces Pombe 317*
Grevbäck	365,296	Ascomcota 26.9 k Basidiomycota 9.5 k	*Botrytis Cinerea 13.9 k* *Sporisorium graminicola 3.61* *Cryptococcus neoformans 1.79 k* *(Candida) glabrata 1.31k* *Rhizoctonia Solani 921*
Vinninga	275,307	Ascomcota 23.8.52 k Basidiomycota 6.52 k	*Saccharomycodes ludwigii 18.2 k* *Sporisorium graminicola 4.55 k* *Puccinia striiformis* 487 *Rhizoctonia Solani 424*

S. Sclerotiorum was found only in the sample when using the Kraken2 databases but not found when analyzed with the UNITE databases. However, many other species of fungi were identified.

Discussion

This study aimed to develop a method to detect *S. sclerotiorum* and other plant pathogens on petals from seven naturally infected oilseed rape fields in Sweden by using a MinIon device from Oxford Nanopore Technologies.

The DNA extraction protocol published by Almquist and Wallenhammar (2014) was used for the isolation of DNA from samples using the MicroLYSIS-PLUS Kit. The purity and concentration of DNA extracted from oilseed rape petals were determined using the NanoDrop and Qubit fluorometer, respectively (Appendix 1 and 2). The obtained concentration of DNA tended to be higher when measured with NanoDrop, which ranged from 86.2 and 245.0 ng/µl compared to 1.15 and 4.68 ng/µl using the Qubit 4 fluorometer. This is a big difference between the two ranges, this result reflects the results obtained by Masago et al. (2021), the accuracy of Qubit assays is generally considered more reliable compared to NanoDrop measurements. Qubit assays utilize fluorescent dyes that specifically bind to nucleic acids, allowing for more precise and accurate quantification of DNA or RNA. In contrast, NanoDrop spectrophotometers rely on the Beer-Lambert equation to estimate nucleic acid concentration based on absorbance at 260 nm, which can lead to overestimation in certain cases. When measuring samples with NanoDrop, the measurement error can range from 1% to 5% when compared to more accurate methods such as Qubit (Sah et al., 2013). This discrepancy is especially noticeable when dealing with samples containing fragmented DNA or contaminants that absorb at 260 nm, such as RNA, proteins, and phenols (Simbolo et al., 2013). NanoDrop's reliance on the Beer-Lambert equation without considering specific sample properties can result in an overestimation of nucleic acid concentration. To obtain more trustworthy and accurate information, Qubit assays are often preferred over NanoDrop measurements. Qubit assays offer better precision and specificity, particularly in cases where sample integrity or contamination may be a concern. Using Qubit assays can help ensure more reliable measurements, especially when working with low DNA concentrations or samples prone to degradation or contamination.

According to Pankoke et al. (2021), an A_{260}/A_{280} ratio of ~1.8 is generally accepted as "pure" for DNA, and the extracted DNA from samples from the seven fields had A_{260}/A_{280} ratios between 2.06 and 2.82. This indicated that the samples were highly contaminated; A_{260}/A_{280} ratios above and below 1.8 and 2.0 suggest RNA and protein contamination, respectively (Glasel, 1995; Wilfinger et al., 2006). To remove the possible contaminant RNA, samples were treated with RNAse A, and the result after being treated with RNAse A was A_{260}/A_{280} ratios between 1.28 and 1.7. These values were also lower than the desired values, which should be around (~1.8), as the findings suggested (Pankoke et al., 2021). Also, the A_{260}/A_{230} ratios range between 0.43 and 0.86 for samples not being treated with RNAse and between 0.30 and 0.63 after being treated with RNAse A. Again numbers were lower than the desired range. The acceptable range for the A_{260}/A_{230} ratio is 1.8 to 2.2, according to Sambrook and Russell (2006). The observed decrease in A_{260}/A_{280} and A_{260}/A_{230} ratios after RNAse A treatment suggests potential DNA degradation during the treatment, as supported by previous findings (Donà & Houseley, 2014). However, it is important to consider other factors that could contribute to the lower ratios, such as contamination and the presence of inhibitors. Contamination is a common concern in molecular biology experiments and can lead to inaccurate and unreliable results. During sample preparation or when opening tubes, cross-contamination can occur, releasing tiny drops into the air, potentially introducing foreign DNA into the samples (Corless et al., 2000). Contaminants can affect the DNA concentration and purity measurements, leading to lower A_{260}/A_{280} and A_{260}/A_{230} ratios.

Inhibitors present in the samples can also cause lower DNA concentrations and affect the ratio measurements. These inhibitors can interfere with DNA polymerase activity, reducing PCR efficiency and resulting in lower target DNA quantity and potential false negatives (Olson & Morrow, 2012). Additionally, the low DNA concentrations themselves can influence the ratio results. As the concentration of DNA decreases, the impact of impurities or contaminants in the sample becomes more prominent compared to the DNA signal. This can result in lower A_{260}/A_{230} ratios, as contaminants or impurities in the sample contribute more significantly to the absorbance in the A230 region (Vogelstein & Gillespie, 1979). Considering these factors, it is important to carefully evaluate the potential causes of the lower A_{260}/A_{280} and A_{260}/A_{230} ratios, taking into account the possibility of DNA degradation, contamination, and the presence of inhibitors. Conducting appropriate controls and following good laboratory practices can help mitigate these issues and ensure reliable and accurate results

Over the last two decades, molecular discovery and characterization of fungi have outperformed traditional morphological descriptions, with public sequence databases accumulating internal transcribed spacer (ITS) barcodes (Schoch et al., 2012). Because the ITS sections of nuclear rDNA change rather quickly, they are highly variable, displaying variances across closely related species and, in some cases, within species (Ward & Adams, 1998; Ward & Bateman, 1999). As a result, the ITS region is an excellent choice for developing specialized PCR primers. Furthermore, because rDNA is present in many copies in most fungal genomes, PCR tests that amplify rDNA should be more sensitive than those directed at single-copy genes. DNA barcoding based on the nucleotide sequence information of a target gene region can be highly efficient in cataloging numerous fungal species and thereby establishing reference databases of fungal variety, potentially enabling the rapid and accurate identification of fungal specimens (Seifert, 2009). To see if *S. sclerotiorum* might be found in DNA isolated from petal samples, the ITS region of fungal DNA was amplified using the primer pairs ITS1Catta and ITS4ngsUni, which were developed particularly by (Toju et al., 2012; Loit et al., 2019) to target the ITS regions of three major fungal phyla: Ascomycota, Basidiomycota, and Zygomycetes.

In order to analyze the PCR products, they were visualized on an agarose gel. To optimize the PCR, the annealing temperature and the number of amplification cycles were adjusted. All seven DNA samples were used to determine the optimal annealing temperature. Several different annealing temperatures were tested and compared, ranging from 55°C to 63.2°C. The expected sizes of the amplified fungal DNA bands on the agarose gel were predicted to be between 400 and 900 base pairs (bp) according to previous studies (Kress & Erickson, 2012). The goal was to identify an annealing temperature that would yield clear, well-defined bands within this size range. Through gel electrophoresis, a very clear band with a size of 700 bp was observed at an annealing temperature of 58.5°C (data not shown). This band fell within the expected amplicon size range of 400-900 bp, considering the natural variability among fungal species (Kress & Erickson, 2012). Hence, the optimal annealing temperature for this PCR reaction was determined to be 58.5°C based on the visualized bands. It is worth noting that the finding regarding the optimal annealing temperature in this research contradicts the results reported by Lum Bongam (2022) and Loit et al. (2019), where they identified 55°C as the best annealing temperature for the same primer pairs used in this study. This discrepancy suggests that different PCR conditions and sample characteristics can influence the optimal annealing temperature required for successful amplification. After determining the optimal annealing temperature, a PCR was performed on all seven DNA samples using the primer pairs ITS1Catta and ITS4ngsUni.

The results obtained from the agarose gel analysis showed that only two samples exhibited a band size of approximately 700 base pairs (Figure 2), while several additional bands were also detected. These additional bands can be attributed to various factors, as discussed by Garibyan and Avashia (2013). There are potential causes for these additional bands. In this study, the number of cycles increased from 35 to 40. Increasing the number of cycles can generally result in a higher quantity of PCR products, as more rounds of amplification lead to an exponential increase in the target DNA. However, it is important to consider the limitations and potential drawbacks of excessive amplification cycles. As highlighted by Lorenz (2012), prolonged amplification can lead to the enrichment of undesired secondary products, such as primer dimers or nonspecific amplification products. These secondary products can appear as additional bands on the agarose gel, which may complicate the interpretation of the results. However, all these results were expected and correspond to the findings reported by Tabussum (2023). Tabussum used an annealing temperature of 55.2°C, which produced clear bands and was determined to be the most suitable annealing temperature for the same primer pairs employed in this study. This alignment with the expected amplicon size range of 400 to 900 base pairs further supports the reliability of the results.

According to Tedersoo (2017), the incorporation of molecular methods into fungal morphological taxonomy has greatly benefited the recognition of fungal species differentiation; therefore, the advanced molecular technique, Nanopore Sequencing, was used for fungal identification in this study. The choice of reference database for nanopore sequence analysis can influence the results obtained. In this study, two databases were utilized: the Kraken2 database and the UNITE database. The result showed that fungus species identified were not the same. When using the reference database (Kraken2), not only fungi species were classified, but a small percentage of sequences were classified under the Viridiplantae kingdom (Figure 3), which is not expected since the Kraken2 database only contained fungal sequences from NCBI's RefSeq. This result is opposite the previous one conducted by Herrera Hernandez (2023). However, when analyzing the sequences using the UNITE database, the results were very different; only fungus species were identified (Table 5). These results were expected since the UNITE database includes fungal ITS sequences from both the UNITE and INSDC databases. Many factors could have a role in this outcome. Petersen et al. (2019) mientioned that the sensitivity and specificity of the analysis, affecting accuracy and reliability, are impacted by the reference database used. It is important to note that reference databases can vary in terms of genome representation, with some being more comprehensive and others more limited,and also the differentiation in their quality (Ciuffreda et al., 2021). In this study, while both databases used are considered to be of high quality, the fact that they are distinct databases introduces a source of variation.

The observed prevalence of Ascomycota and Basidiomycota as the most common phyla in all samples (Tables 4 and 5) aligns with the findings reported by Loit et al. (2019) and Siddiq (2023), who also employed the same primer pair in their studies. This consistency across multiple studies using the same primer pair strengthens the reliability and credibility of these results. The presence of these dominant fungal phyla further supports the understanding of their widespread occurrence and importance in the studied sample set.

The pathogen *S. sclerotiorum* was detected solely using the Kraken2 database and not with the UNITE database . The absence of *S. sclerotiorum* in the results obtained using the UNITE database despite using the same sequences as the Kraken2 database is intriguing. One possible explanation

could be differences in the databases' coverage or representation of *S. sclerotiorum* sequences. It is possible that the UNITE database lacks or has limited representation of *S. sclerotiorum* sequences, leading to its non-detection as stated by Ciuffreda et al. (2021). This highlights the importance of considering the comprehensiveness and quality of reference databases in order to capture the diversity of fungal species accurately.

Furthermore, the significant variation observed in the identification of other fungal species between the databases suggests differences in their content and annotations. Reference databases can differ in terms of the included species, their genome coverage, and the quality of annotations. These factors can influence the ability to accurately identify and classify fungal species. It is crucial to carefully assess the databases used and consider their limitations when interpreting results (Petersen et al., 2019). To further elucidate the reasons behind the observed variations, it would be beneficial to investigate the specific sequences used in both databases and compare their representation of known *S. sclerotiorum* and other fungal species. Additionally, exploring alternative reference databases or integrating multiple databases may provide a more comprehensive view of the fungal community and help uncover potential discrepancies in species identification (Petersen et al., 2019). The differences in results, when different databases and tools were utilized, could lead to considerable differences in the classification of distinct biological taxa, characterization of community structures, and identification of differentially abundant species. The main causes of these inconsistencies are differences in database content and read profiling methods, as stated by Xu et al. (2023). Another thing is that the *S. sclerotiorum* found only in one of the samples, but not the other ones. It is possible that the *S. sclerotiorum* pathogen was not present in the samples used for sequencing, which could explain its absence in the results of other samples. This discrepancy is unexpected and warrants further investigation to understand the underlying reasons for this disparity.

In addition to *S. sclerotiorum*, the reference databases Kraken2 and UNITE identified other important fungal pathogens affecting rapeseed crops in Sweden (Table 4 and 5). *Alternaria brassicicola* and *Fusarium spp*. were found to be prevalent, which is consistent with the study conducted by Herrera Hernandez (2023). Another significant pathogen detected was *Botrytis cinerea*, known for causing gray mold diseases and resulting in substantial losses, particularly in crops like wine grapes. This necrotrophic fungus was also anticipated and aligns with the findings of Loit et al. (2019) and Siddiq (2023). Furthermore, the UNITE database revealed the presence of several other fungal species that were frequently detected across all samples. Among them, *S. ludwigii*, belonging to the Saccharomycodaceae family, is known for its ability to spoil wine and its high tolerance to sulfur dioxide, as mentioned by Tavares et al. (2021). Additionally, the study by Wu et al. (2022) highlighted the significant yield losses caused by *Puccinia striiformis*, a fungal pathogen affecting wheat production worldwide.

Conclusion

In conclusion, the study successfully utilized MinIon nanopore sequencing to identify the target fungus *S. sclerotiorum* in one field when analyzed with Kraken2. However, in the remaining four samples of oilseed rape petals, it is possible that the *S. sclerotiorum* pathogen was not present, suggesting potential variability across the samples. The sequencing results also revealed the detection of other fungal species with a high number of reads, including representatives from the Ascomycota and Basidiomycota phyla. While these additional species were identified, the specific aim of the study, which was to identify *S. sclerotiorum* from oilseed rape petals using nanopore sequencing, was successfully achieved. Overall, the study demonstrates the feasibility and effectiveness of nanopore sequencing for targeted pathogen identification, highlighting its potential utility in fungal pathogen detection and characterization in oilseed rape and similar agricultural systems.

Ethical aspects and impact on the society

All genetic material used in the present study was obtained from oilseed rape fields in the northeastern area of Sweden. There was no personal information attached to the petal samples. All conclusions in this study were based on theories underlying recognized and referenced scientific procedures. This study was funded by the University of Skövde. All data processing and analysis tools were freely available as open source. This study's findings and conclusions were entirely based on the experimental data collected. The research detailed in this essay explores plant infections of plant fungi and their ethical effects, which may have an impact on society. therefore, ethics education and sensitization of society in general, and plant researchers in particular, is a critical issue**.** *Sclerotinia sclerotiorum* is a common plant pathogen with agricultural and economic importance around the world. The infection by *S. sclerotiorum* causes a lot of losses to important economic crops. This relevance underscores the importance of good disease control measures, such as crop rotation with non-host crops, growing cultivars with some tolerance, and employing appropriate chemical practices.

The early detection of fungal pathogens can help farmers make more informed decisions regarding the use of fungicides and reduce the number of unnecessary fungicide applications. Using fungicides is one of the most common strategies to protect crops from this infection. The cultivators usually use fungicides in amounts that are excessive or unnecessary, which can affect the environment, especially the human, plant, and animal species, and this important ethic will need to be considered. Managing molecular techniques through research and developing the techniques to detect this pathogen will help minimize the use of fungicides and reduce crop loss. The use of MinION nanopore sequencing can provide more precise and accurate data on the existence of a fungal being present allowing farmers to take proactive measures to manage fungal infections in their fields. Avoiding these losses will enable increased rape oil production and, as a result, lower rape oil pricing because farmers will not waste their fungicide applications. Furthermore, if the fungi are not found in the plant, there is no need for fungicide applications, which would substantially contribute to the preservation of the environment. Growing concern about the environmental and human health effects of pesticides in general and fungicides and herbicides, in particular, has forced the development of alternative farming approaches. In general, the current study emphasizes the importance of additional research to optimize and

improve the application of MinION Nanopore sequencing for detecting fungal infections in crops, which can have significant consequences for sustainable agriculture and food security.

Future Perspectives

The unique features of the MinION nanopore sequencer, including its portability, cost-effectiveness, and real-time data generation, have revolutionized phytopathogen diagnosis approaches in scientific research (Phannareth et al., 2021; Xu et al., 2021; Marcolungo et al., 2022). These characteristics also make the nanopore sequencer an attractive option for future diagnostic technological advancements. Based on the aforementioned analysis, several future approaches can be considered to enhance the identification of *S. sclerotiorum*. Exploring different DNA extraction kits and utilizing multiple kits can be explored to improve resolution and accuracy in identification. By comparing the results obtained from different kits, a clearer understanding of the pathogen's presence can be achieved. Additionally, the integration of nano-scale electronics can contribute to the development of smart agricultural systems with unique capabilities. These nanodevices have the potential to detect plant health issues before they become apparent to growers. They can react to abnormal conditions, identify pathogens, and initiate appropriate disease management measures. Consequently, these miniature smart devices can serve as protective and warning systems. Improvements in bioinformatics analysis of sequencing data are crucial to avoid any discrepancies or misinterpretations. Enhancing the data processing phase by incorporating more sophisticated algorithms and implementing robust quality control procedures can lead to more reliable outcomes. Furthermore, modern data processing approaches such as metagenomic assembly, comparative genomics, and functional annotation can provide valuable additional insights into the identified fungal species.

By integrating these future approaches, the field of phytopathogen diagnosis can further benefit from the capabilities of the MinION nanopore sequencer, leading to enhanced accuracy, efficiency, and understanding of plant pathogens.

Acknowledgments

I express my deepest gratitude to Allah Almighty for His blessings and guidance throughout my study. I would like to extend my sincere appreciation to the Swedish Institute scholarship committee for selecting me for this prestigious opportunity to pursue my education at a renowned university in Sweden. I am immensely grateful to my supervisor, Dr. Maria Algerin, for her invaluable guidance, support, and kind treatment throughout the duration of my research. I would also like to thank my examiner, Dr. Magnus Fagerlind, for his valuable insights and feedback. I extend my heartfelt thanks to my co-supervisors, Johan Nordén and John Baxter, for their assistance and support during the experimental work and data analysis. Their expertise and guidance were instrumental in the success of this study. Additionally, I am grateful to my family and friends for their unwavering support and prayers throughout my academic journey. Their encouragement and belief in me have been a constant source of motivation. Once again, I express my sincerest appreciation to all those who have contributed to the realization of this study and my personal growth.

References

Abd-Elmagid, A., Garrido, P. A., Hunger, R., Lyles, J. L., Mansfield, M. A., Gugino, B. K., ... & Garzon, C. D. (2013). Discriminatory simplex and multiplex PCR for four species of the genus Sclerotinia. *Journal of Microbiological Methods*, *92*(3), 293-300.

Bellemain, E., Carlsen, T., Brochmann, C., Coissac, E., Taberlet, P., & Kauserud, H. (2010). ITS as an environmental DNA barcode for fungi: an in silico approach reveals potential PCR biases. *BMC microbiology*, *10*, 1-9.

Bolton, M. D., Thomma, B. P., & Nelson, B. D. (2006). *Sclerotinia sclerotiorum* (Lib.) de Bary: biology and molecular traits of a cosmopolitan pathogen. *Molecular plant pathology*, *7*(1), 1-16.

Bom, M., & Boland, G. J. (2000). Evaluation of polyclonal-antibody-based immunoassays for detection of Sclerotinia sclerotiorum on canola petals, and prediction of stem rot. *Canadian journal of microbiology*, *46*(8), 723-729.

Ciuffreda, L., Rodríguez-Pérez, H., & Flores, C. (2021). Nanopore sequencing and its application to the study of microbial communities. *Computational and structural biotechnology journal*, *19*, 1497-1511.

Clarkson, J. P., Staveley, J., Phelps, K., Young, C. S., & Whipps, J. M. (2003). Ascospore release and survival in Sclerotinia sclerotiorum. *Mycological Research*, *107*(2), 213-222.

Corless, C. E., Guiver, M., Borrow, R., Edwards-Jones, V., Kaczmarski, E. B., & Fox, A. J. (2000). Contamination and Sensitivity Issues with a Real-Time Universal 16S rRNA PCR. Journal of Clinical Microbiology, 38(5), 1747–1752.

Cornelis, S., Gansemans, Y., Vander Plaetsen, A. S., Weymaere, J., Willems, S., Deforce, D., & Van Nieuwerburgh, F. (2019). Forensic tri-allelic SNP genotyping using nanopore sequencing. *Forensic Science International: Genetics*, *38*, 204-210.

Coughlan, R., Moane, S., & Larkin, T. (2022). Variability of essential and nonessential fatty acids of Irish rapeseed oils as an indicator of nutritional quality. *International Journal of Food Science*, *2022*.

Donà, F., & Houseley, J. (2014). Unexpected DNA loss mediated by the DNA binding activity of ribonuclease A. *PLoS One*, *9*(12), e115008.

Freeman, J., Ward, E., Calderon, C., & McCartney, A. (2002). A polymerase chain reaction (PCR) assay for the detection of inoculum of *Sclerotinia sclerotiorum*. *European Journal of Plant Pathology*, *108*, 877-886.

Garibyan, L., & Avashia, N. (2013). Polymerase Chain Reaction. *Journal of Investigative Dermatology*, *133*(3), 1–4.

Glasel, J. A. (1995). Validity of nucleic acid purities monitored by 260nm/280nm absorbance ratios. *Biotechniques*, *18*(1), 62-63.

Goldstein, S., Beka, L., Graf, J., & Klassen, J. L. (2019). Evaluation of strategies for the assembly of diverse bacterial genomes using MinION long-read sequencing. *BMC genomics*, *20*(1), 1-17.

Gugel, R. K. (1986). Inoculum-disease relationships in Sclerotinia stem rot of rapeseed in Saskatchewan. *Canadian Journal of Plant Pathology*, *8*(1), 89-96.

Gül, M. K., & Amar, S. (2006). Sterols and the phytosterol content in oilseed rape (Brassica napus L.). *Journal of Cell & Molecular Biology*, *5*(2).

Gunstone, F. D. (2001). Production and consumption of rapeseed oil on a global scale. *Eur. J. Lipid Sci. Technol.*, *103*, 447-449.

Heran, A., McCartney, H. A., & Li, Q. (1999, September). The effect of petal characteristics, inoculum density, and environmental factors on infection of oilseed rape by *Sclerotinia sclerotiorum*. In *Proceedings of the 10th International Rapeseed Congress-New Horizons for an Old Crop, Canberra*.

Herrera Hernandez, A. G. (2023). Detection of Sclerotinia sclerotiorum in oilseed rape using Oxford Nanopore sequencing and qPCR.

Ip, C. L., Loose, M., Tyson, J. R., de Cesare, M., Brown, B. L., Jain, M. (2015). MinION Analysis and Reference Consortium: Phase 1 data release and analysis. *F1000Research*, *4*.

Jamaux, I., Gélie, B., & Lamarque, C. (1995). Early stages of infection of rapeseed petals and leaves by *Sclerotinia sclerotiorum* revealed by scanning electron microscopy. *Plant Pathology*, *44*(1), 22-30.

Jansen, H. J., Liem, M., Jong-Raadsen, S. A., Dufour, S., Weltzien, F. A., Swinkels, W., ... & Henkel, C. V. (2017). Rapid de novo assembly of the European eel genome from nanopore sequencing reads. *Scientific reports*, *7*(1), 7213.

Koch, S., Dunker, S., Kleinhenz, B., Röhrig, M., & Tiedemann, A. V. (2007). A crop loss-related forecasting model for Sclerotinia stem rot in winter oilseed rape. *Phytopathology*, *97*(9), 1186-1194.

Kress, W.J., Erickson D.L. (2012). DNA Barcodes: Methods and Protocols. In: Kress W., Erickson D. (eds) DNA Barcodes. Methods in Molecular Biology (Methods and Protocols*), Humana Press, Totowa, NJ v*ol 858.

Lievens, B., Brouwer, M., Vanachter, A. C., Cammue, B. P., & Thomma, B. P. (2006). Real-time PCR for detection and quantification of fungal and oomycete tomato pathogens in plant and soil samples. *Plant science*, *171*(1), 155-165.

Lin, C. S., Xin, Z. C., Dai, J., & Lue, T. F. (2013). Commonly used mesenchymal stem cell markers and tracking labels: Limitations and challenges. *Histology and histopathology*, *28*(9), 1109.

Lorenz, T. J. (2012). Polymerase Chain Reaction: Basic Protocol Plus Troubleshooting and Optimization Strategies. *Journal of Visualized Experiments*, *63*.

Lum Bongam, A. (2022). Detection Of Soil Borne Pathogens Causing Pea Root Rot Using Minion.

Martin, K. J., & Rygiewicz, P. T. (2005). Fungal-specific PCR primers developed for analysis of the ITS region of environmental DNA extracts. *BMC microbiology*, *5*(1), 1-11.

Masago, K., Fujita, S., Oya, Y., Takahashi, Y., Matsushita, H., Sasaki, E., & Kuroda, H. (2021). Comparison between fluorimetry (Qubit) and spectrophotometry (NanoDrop) in the quantification of DNA and RNA extracted from frozen and FFPE tissues from lung cancer patients: A real-world use of genomic tests. *Medicina*, *57*(12), 1375.

McCartney, H. A., Heran, A., Li, Q., & Foster, S. J. (2001). Infection of oilseed rape (Brassica napus) by petals containing ascospores of *Sclerotinia sclerotiorum*. Proceedings of Sclerotinia, 181–182.

Middleton, J. (2017). Public health in England in 2016—the health of the public and the public health system: a review. *British Medical Bulletin*, *121*(1).

Mikheyev, A. S., & Tin, M. M. (2014). A first look at the Oxford Nanopore MinION sequencer. *Molecular ecology resources*, *14*(6), 1097-1102.

O'brien, R. D. (2008). *Fats and oils: formulating and processing for applications*. CRC press.

Olson, N. D., & Morrow, J. B. (2012). DNA extract characterization process for microbial detection methods development and validation. *BMC research notes*, *5*, 1-14.

Petersen, L. M., Martin, I. W., Moschetti, W. E., Kershaw, C. M., & Tsongalis, G. J. (2019). Third-generation sequencing in the clinical laboratory: exploring the advantages and challenges of nanopore sequencing. *Journal of clinical microbiology*, *58*(1), e01315-19.

Qin, L., Fu, Y., Xie, J., Cheng, J., Jiang, D., Li, G., & Huang, J. (2011). A nested-PCR method for rapid detection of *Sclerotinia sclerotiorum* on petals of oilseed rape (Brassica napus). *Plant pathology*, *60*(2), 271-277.

Reiner, J. E., Balijepalli, A., Robertson, J. W., Campbell, J., Suehle, J., & Kasianowicz, J. J. (2012). Disease detection and management via single nanopore-based sensors. *Chemical reviews*, *112*(12), 6431-6451.

Rogers, S. L., Atkins, S. D., & West, J. S. (2009). Detection and quantification of airborne inoculum of Sclerotinia sclerotiorum using quantitative PCR. *Plant Pathology*, *58*(2), 324-331.

Sambrook, J., & Russell, D. W. (2006). *The condensed protocols from molecular cloning: a laboratory manual*. Cold Spring Harbor Laboratory Press.

Schoch, C. L., Seifert, K. A., Huhndorf, S., Robert, V., Spouge, J. L., Levesque, C. A., ... & White, M. M. (2012). Nuclear ribosomal internal transcribed spacer (ITS) region as a universal DNA barcode marker for Fungi. *Proceedings of the national academy of Sciences*, *109*(16), 6241-6246.

Seifert, K. A., Wingfield, B. D., & Wingfield, M. J. (1995). A critique of DNA sequence analysis in the taxonomy of filamentous Ascomycetes and ascomycetous anamorphs. *Canadian Journal of Botany*, *73*(S1), 760-767.

Siddiq, M. (2023). Analysing rapeseed leaves from naturally infested fields in Skaraborg to detect Sclerotinia sclerotiorum using Nanopore sequencing.

Simbolo, M., Gottardi, M., Corbo, V., Fassan, M., Mafficini, A., Malpeli, G., ... & Scarpa, A. (2013). DNA qualification workflow for next generation sequencing of histopathological samples. *PloS one*, *8*(6), e62692.

Tabussum, L. (2023). Exploring the diversity and distribution of Sclerotinia sclerotiorum in oilseed rape through molecular techniques.

Tavares, M. J., Güldener, U., Mendes-Ferreira, A., & Mira, N. P. (2021). Genome sequencing, annotation and exploration of the SO2-tolerant non-conventional yeast Saccharomycodes ludwigii. *BMC genomics*, *22*(1), 1-15.

Toju, H., Tanabe, A. S., Yamamoto, S., & Sato, H. (2012). High-coverage ITS primers for the DNA-based identification of ascomycetes and basidiomycetes in environmental samples. *PloS one*, *7*(7), e40863.

Turkington, R., Hamilton, R. S., & Gliddon, C. (1991). Within-population variation in localized and integrated responses of Trifolium repens to biotically patchy environments. *Oecologia*, *86*, 183-192.

Twengstrom, E., Sigvald, R., Svensson, C., & Yuen, J. (1998). Forecasting Sclerotinia stem rot in spring-sown oilseed rape. *Crop Protection*, *17*(5), 405-411.

Vogelstein, B., & Gillespie, D. (1979). Preparative and analytical purification of DNA from agarose. *Proceedings of the National Academy of Sciences*, *76*(2), 615-619.

Wallenhammar, A. C., Almquist, C., Schwelm, A., Roos, J., Marzec-Schmidt, K., Jonsson, A., & Dixelius, C. (2014). Clubroot, a persistent threat to Swedish oilseed rape production. *Canadian Journal of Plant Pathology*, *36*(sup1), 135-141.

Wallenhammar, A. C., Almquist, C., Soderstrom, M., & Jonsson, A. (2012). In-field distribution of Plasmodiophora brassicae measured using quantitative real-time PCR. *Plant Pathology*, *61*(1), 16-28.

Wallenhammar, A. C., Sjoberg, A., & Redner, A. (2007, March). Development of methods improving the precision of risk assessment of Sclerotinia stems rot in oilseed rape. In *Proceedings of the 12th International Rapeseed Congress, Wuhan, China* (pp. 112-5). Monmouth Junction: GCIRC.

Wilfinger, W. W., Mackey, K., & Chomczynski, P. (2006). Assessing the quantity, purity and integrity of RNA and DNA following nucleic acid purification. *DNA sequencing II optimizing preparation and cleanup*, *291*, 312.

Willetts, H. J., & Wong, J. A. L. (1980). The biology of Sclerotinia sclerotiorum, S. trifoliorum, and S. minor with emphasis on specific nomenclature. *The Botanical Review*, *46*, 101-165.

Wood, D. E., & Salzberg, S. L. (2014). Kraken: ultrafast metagenomic sequence classification using exact alignments. *Genome biology*, *15*(3), 1-12.

Wu, N., Ozketen, A. C., Cheng, Y., Jiang, W., Zhou, X., Zhao, X., ... & Akkaya, M. S. (2022). Puccinia striiformis f. sp. tritici effectors in wheat immune responses. *Frontiers in Plant Science*, *13*, 1012216.

Wurzbacher, C., Larsson, E., Bengtsson-Palme, J., Van den Wyngaert, S., Svantesson, S., Kristiansson, E. (January 2019). "Introducing ribosomal tandem repeat barcoding for fungi". *Molecular Ecology Resources*. 19 (1): 118– 127. doi:10.1111/1755-0998.12944.

Xu, R., Rajeev, S., & Salvador, L. C. (2023). The selection of software and database for metagenomics sequence analysis impacts the outcome of microbial profiling and pathogen detection. *Plos one*, *18*(4), e0284031.

Appendix

Appendix 1- result before being treated with RNAse A

The NanoDrop and Qubit results for pulled-up DNA samples Before being treated with RNAse A.

Fields	Absorbance 260/280	Absorbance 260/230	NanoDrop concentration (ng/µl)	Qubit concentration (ng/µl)
Ova	2.82	0.43	86.2	1.26
Kaflås	2.06	0.76	159.1	1.15
Dala	2.08	0.78	187.0	2.92
Hovby	2.24	0.78	217.5	4.14
Grevbäck	2.54	0.86	245.0	2.98
Forsby	2.11	0.75	182.8	3.26
Vinninga	2.33	0.83	283.5	4.68

The expected 260/280 value is ~1.8 and is generally accepted as pure for DNA. Expected 260/230 values are commonly in the range of 2.0-2.2.

Appendix 2- result after being treated with RNAse A

The NanoDrop and Qubit results of pulled-up DNA samples collected from seven infected fields After being treated with RNAse A (25 mg/mL).

Fields	Absorbance 260/280	Absorbance 260/230	NanoDrop concentration (ng/µl)	Qubit concentration (ng/µl)
Ova	1.38	0.30	193.1	0.72
Kaflås	1.40	0.33	190.2	1.55
Dala	1.28	0.63	245.5	1.60
Hovby	1.52	0.39	232.4	2.10
Grevbäck	1.77	0.42	243.4	2.02
Forsby	1.28	0.30	190.6	1.79
Vinninga	1.66	0.46	294.3	1.51

The expected 260/280 value is ~1.8 and is generally accepted as pure for DNA. Expected 260/230 values are commonly in the range of 2.0-2.2.